Inorg. Chem. **2003**, *42*, 8465–8475

New Dicationic Porphyrin Ligands Suited for Intercalation into B-Form DNA

Stephanie A. Bejune, Alexander H. Shelton, and David R. McMillin*

Department of Chemistry, Purdue University, 560 Oval Drive, West Lafayette, Indiana 47907-2084

Received September 16, 2003

This paper describes the synthesis and characterization of a new series of sterically nondemanding, dicationic porphyins that exhibit novel DNA-binding interactions. Cationic porphyrins continue to be the focus of a great deal of effort because of the promise they have for use in photodynamic, antiviral, and anticancer therapies. The systems explored here include 5,15-di(*N*-methylpyridinium-4-yl)porphyrin (H_2D4), 5,15-di(*N*-methylpyridinium-3-yl)porphyrin (H_2D3), and 5,15-di(*N*-methylpyridinium-2-yl)porphyrin (H_2D2), as well as Zn(D4) and Zn(D3), the zinc(II)-containing derivatives of H_2D4 and H_2D3, respectively. Viscometry studies, in conjunction with various spectroscopic techniques, reveal the nature of the adducts formed with DNA. Irrespective of the base composition, H_2D4 and H_2D3 bind to DNA by intercalation. The zinc derivatives Zn(D4) and Zn(D3) are also intercalators; however, the binding constants are smaller because uptake requires the loss of an axial ligand. The decisive roles that steric factors and structural rigidity play in shaping the adducts with DNA become clear. Sequences that contain mainly adenine–thymine base pairs easily depart from the canonical B-form DNA structure and generally accommodate bulky porphyrins in external binding sites. However, with the H_2D3 and H_2D4 systems, the steric requirements are so minimal that intercalation becomes the preferred mode of binding, even in [poly(dA–dT)]$_2$. The intercalated form of the H_2D2 isomer is less stable, probably because of frontal strain associated with the (*N*-methyl)pyridinium-2-yl groups. A qualitative energy-level diagram is useful for assessing the forces that influence binding and could guide the design of new porphyrin ligands.

Introduction

The cationic chromophore 5,10,15,20-tetra(*N*-methylpyridinium-4-yl)porphyrin, or H_2T4 in Scheme 1, has been the focus of a great deal of attention. It is water soluble and has a natural Coulombic attraction for DNA that Fiel and coworkers first exploited.[1] By now, there are many extensive reviews that deal with this chemistry.[2−5] In vivo, cationic porphyrins appear to enter cells via pinocytosis,[6] and there is evidence that they tend to accumulate in mitochondria.[7] Potential therapeutic and clinical applications of porphyrins abound. Due to the strong visible absorption in the red, early studies focused on photodynamic therapy.[8−11] Ions such as H_2T4 and some of its derivatives also exhibit antiviral activity.[12,13] Because these same cations bind to telomeric DNA, they also act as inhibitors of telomerase, an enzyme that has a significant role in extending the life of tumor cells.[14,15]

The H_2T4 system is also interesting because the mode of binding varies with the composition of the DNA host.[3−5,16]

* Corresponding author. Fax: (765) 494-0239. E-mail: mcmillin@purdue.edu.

(1) Fiel, R. J.; Howard, J. C.; Mark, E. H.; Dattagupta, N. *Nucleic Acids Res.* **1979**, *6*, 3093−3118.
(2) Fiel, R. J. *J. Biomol. Struct. Dyn.* **1989**, *6*, 1259−1275.
(3) Marzilli, L. G. *New J. Chem.* **1990**, *14*, 409−420.
(4) Pasternack, R. F.; Gibbs, E. J. *Met. Ions Biol. Syst.* **1996**, *33*, 367−397.
(5) McMillin, D. R.; McNett, K. M. *Chem. Rev.* **1998**, *98*, 1201−1219.
(6) Ruck, A.; Steiner, R. *Minim. Invasive Ther. Allied Technol.* **1998**, *7*, 503−509.
(7) Spizzirri, P. G.; Hill, J. S.; Kahl, S. B.; Ghiggino, K. P. *Photochem. Photobiol.* **1996**, *64*, 975−983.
(8) Henderson, B. W.; Dougherty, T. J. *Photochem. Photobiol.* **1992**, *55*, 145−157.
(9) Ali, H.; van Lier, J. E. *Chem. Rev.* **1999**, *99*, 2379−2450.
(10) Ackroyd, R.; Kelty, C.; Brown, N.; Reed, M. *Photochem. Photobiol.* **2001**, *74*, 656−669.
(11) Lane, N. *Sci. Am.* **2003**, *288* (1), 38−45.
(12) Dixon, D. W.; Schinazi, R.; Marzilli, L. G. *Ann. N. Y. Acad. Sci.* **1990**, *616*, 511−513.
(13) Kasturi, C.; Platz, M. S. *Photochem. Photobiol.* **1992**, *56*, 427−429.
(14) Han, F. X. G.; Wheelhouse, R. T.; Hurley, L. H. *J. Am. Chem. Soc.* **1999**, *121*, 3561−3570.
(15) Cech, T. R. *Angew. Chem., Int. Ed.* **2000**, *39*, 35−43.

10.1021/ic035092i CCC: $25.00
Published on Web 10/28/2003

Scheme 1

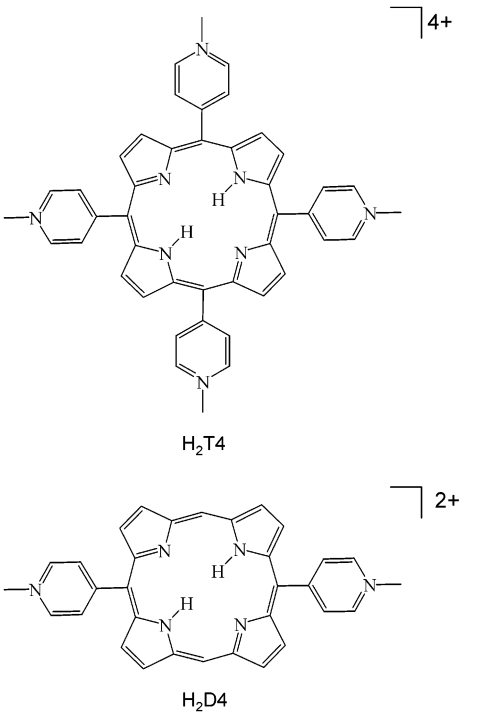

DNA sequences which are rich in guanine−cytosine (G≡C) base pairs support intercalative binding. Spectroscopic consequences in the Soret region include a strong bathochromic shift ($\Delta\lambda \geq 15$ nm), marked hypochromism ($H \geq 35\%$), and an induced circular dichroic (CD) signal with a negative amplitude.[3,5,17] In contrast, DNA sequences that are rich in adenine−thymine (A=T) base pairs support external binding, in which case the Soret band undergoes a smaller bathochromic shift ($\Delta\lambda \leq 8$ nm), shows weaker hypochromism ($H \leq 10\%$), and gives an induced CD signal with the opposite sign.[17] There are two structures available for intercalated porphyrins,[18,19] and another which reveals an external, groove-binding interaction.[20] However, the relevance to solution work is not entirely clear because the two X-ray structures both define porphyrins that simultaneously interact with two duplexes in the lattice.[18,20]

In addition to attractive forces, the importance of steric interactions in shaping the DNA-binding interactions has become increasingly apparent. The first effect to come to light was the periplanar, i.e., out-of-plane, nature of the pyridinium substituents.[21] The extreme example is H_2T2, or 5,10,15,20-tetra(*N*-pyridinium-2-yl)porphyrin, which binds only externally to DNA, regardless of the base sequence. The original thinking was that H_2T2 does not intercalate because the pyridine rings cannot even transiently rotate into the plane of the porphyrin.[1] Pasternack and co-workers later emphasized that metal derivatives of H_2T4 are also incapable of intercalating if the metal center retains one or more axial ligands.[17] Calculations by Ford et al. led to the proposal that clashes between thymine methyls and the pyridinium groups of H_2T4 inhibit intercalation within a 5′-ApT-3′ step,[22] but later base-replacement studies did not confirm this effect.[16] Recently, structural studies by Lipscomb et al. identified crucial steric effects that occur whenever a tetrapyridyl porphyrin intercalates. The strain occurs in the minor groove where pyridinium groups of the porphyrin clash with the sugar−phosphate backbone of DNA.[18] External binding is not always high affinity either, as it requires a structural reorganization (partial melting) of B-form DNA to create an optimal binding pocket.[5,16,23−25]

A major breakthrough came with the recent synthesis of a less bulky dipyridyl porphryin H_2D3, or 5,15-di(*N*-methylpyridinium-3-yl)porphyrin, the first porphyrin that binds to DNA exclusively by intercalation.[26] The work described below encompasses the new dipyridyl porphyrins, H_2D4 = 5,15-di(*N*-methylpyridinium-4-yl)porphyrin (Scheme 1) and H_2D2 = 5,15-di(*N*-methylpyridinium-2-yl)porphyrin, as well as the zinc(II) derivatives, Zn(D3) and Zn(D4). Extensive studies with an assortment of DNA hosts provide new insights into the balance of forces shaping binding interactions with cationic porphyrins.

Experimental Section

Materials. Sigma-Aldrich Chemical Company supplied pyrrole, pyrrole-2-carbaldehyde, pyridine-2-carbaldehyde, pyridine-4-carbaldehyde, methyl *p*-toluenesulfonate, methyl triflate, propionic acid, [tetra(*N*-methylpyridium-4-yl)porphyrin][tosylate]$_4$, trimethyl phosphate, dichlorodimethylsilane, sodium borohydride, sodium tetrafluoroborate, and Florisil stationary chromatography phase. Chelex 100 resin as well as topoisomerase I and pBR322 DNA came from GibcoBRL, while Sigma-Aldrich supplied the sodium salt of poly(deoxyguanylic−deoxycytidylic) acid ([poly(dG−dC)]$_2$), the sodium salt of poly(deoxyadenylic−deoxythymidylic) acid ([poly(dA−dT)]$_2$), salmon testes (ST) DNA, Trizma HCl, Trizma base, and dithiothreitol (DTT). The phosphate buffer components, $NaH_2PO_4 \bullet H_2O$ and Na_2HPO_4, came from Mallinckrodt as did hexane, acetic acid, acetic anhydride, and ethylenediaminetetracetic acid (EDTA). Integrated DNA Technologies supplied the (hairpin-forming) oligonucleotides 5′-GATTACTTTTGTAATC-3′, 5′-GATAACTTTTGTTATC-3′, and 5′-GACGACTTTTGTCGTC-3′, as well as the 20-mer variant 5′-GACCGGACTTTTGTCCGGTC-3′, to be abbreviated below as TT[T4], TA[T4], CG[T4], and CCGG[T4], respectively. Pharmco supplied ethanol. VWR Scientific Products supplied (Burdick and Jackson) methanol, chloroform,

(16) Thomas, K. E.; McMillin, D. R. *J. Phys. Chem. B* **2001**, *105*, 12628−12633.
(17) Pasternack, R. F.; Gibbs, E. J.; Villafranca, J. J. *Biochemistry* **1983**, *22*, 2406−2414.
(18) Lipscomb, L. A.; Zhou, F. X.; Presnell, S. R.; Woo, R. J.; Peek, M. E.; Plaskon, R. R.; Williams, L. D. *Biochemistry* **1996**, *35*, 2818−2823.
(19) Guliaev, A. B.; Leontis, N. B. *Biochemistry* **1999**, *38*, 15425−15437.
(20) Bennett, M.; Krah, A.; Wien, F.; Garman, E.; McKenna, R.; Sanderson, M.; Neidle, S. *Proc. Natl. Acad. Sci. U.S.A.* **2000**, *97*, 9476−9481.
(21) Carvlin, M. J.; Fiel, R. J. *Nucleic Acids Res.* **1983**, *11*, 6121−6139.
(22) Ford, K.; Fox, K. R.; Neidle, S.; Waring, M. J. *Nucleic Acids Res.* **1987**, *15*, 2221−2234.
(23) Raner, G.; Goodisman, J.; Dabrowiak, J. C. *ACS Symp. Ser.* **1989**, No. 402, 74−89.
(24) Gibbs, E. J.; Maurer, M. C.; Zhang, J. H.; Reiff, W. M.; Hill, D. T.; Malickablaszkiewicz, M.; McKinnie, R. E.; Liu, H. Q.; Pasternack, R. F. *J. Inorg. Biochem.* **1988**, *32*, 39−65.
(25) Tears, D. K. C.; McMillin, D. R. *Chem. Commun.* **1998**, 2517−2518.
(26) Wall, R. K.; Shelton, A. H.; Bonaccorsi, L. C.; Bejune, S. A.; Dube, D.; McMillin, D. R. *J. Am. Chem. Soc.* **2001**, *123*, 11480−11481.

and dichloromethane (DCM), as well as 1-propanol, while deuterated chloroform ($CDCl_3$) came from Cambridge Isotope Labs. Other suppliers were Bethesda Research Labs for agarose, Glen Research Corporation for Poly-Pak columns, and Millipore Corporation for 0.22 μm filters. John Anderson of Purdue University generously provided ethidium bromide, and the zinc(II) derivative of 5,15-di-(*N*-methylpyridinium-3-yl)porphyrin, or Zn(D3), was available from a previous study.[26]

Synthesis. The basic strategy for porphyrin synthesis resembles the one used previously for the preparation of H_2D3n (5,15-di-(pyrid-3-yl)porphyrin) and the dicationic derivative, H_2D3 (5,15-di(*N*-methylpyridinium-3-yl)porphyrin).[26] The procedures reported below include all modifications.

Dipyrromethane: A combination of literature methods provided convenient access to dipyrromethane (DPM).[27,28] The desired product formed after heating a 20-fold excess pyrrole together with formalin in a 50:50 acetic acid/methanol mixture. The original product was a viscous oil isolated after evaporation of solvent and excess reagents. After extraction into hot hexane, solid deposited on cooling. The ^{1}H NMR spectrum of the product confirmed that DPM was present and that the purity was adequate for porphyrin synthesis.

H_2D4n (5,15-Di(pyrid-4-yl)porphyrin): The method of porphyrin synthesis derived from many sources.[29−32] A typical reaction mixture consisted of 100 mL of propionic acid, 10 mL of acetic anhydride, 15 mL of nitrobenzene, 4.0 mmol of pyridine-4-carbaldehyde, and about 3 mmol of DPM. The next step was heating in air to near boiling in a microwave oven followed by cooling. Usually there were a total of four or five heating/cooling cycles of this type, and the mixture became very dark even by the end of the first cycle. Subsequent removal of about half of the solvent by distillation under aspirator vacuum facilitated extraction of the porphyrin. Addition by turns of aqueous base, typically phosphate, carbonate, or hydroxide, and dichloromethane ultimately produced two layers. When neutralization and washing was complete, it was possible to remove some of the tar by batch extraction with alumina or Florisil. An oily residue remained after separation from the resin and evaporation of solvent. Another wash with an aqueous phosphate buffer sometimes improved the loading properties for subsequent chromatography. Step elution with a DCM/methanol mobile phase by gravity-driven or flash chromatography on Florisil then yielded at least three porphyrin-related products. After application of a couple column volumes of DCM, elution with 1% methanol yielded the first pigmented fraction containing the monopyridyl product, 5-(pyrid-4-yl)porphyrin. The desired product 5,15-di(pyrid-4-yl)porphyrin, or H_2D4n, eluted in 2% methanol. A product with a chlorin-like visible absorption spectrum followed closely. Other dark material remained on the column. Evaporation of the desired middle fraction gave purple crystals of partially solvated solid. Calcd for $C_{30}H_{20}N_6 \cdot {}^1/_2CH_3OH \cdot {}^1/_4CH_2Cl_2$: 73.60% C, 4.51% H, 16.74% N. Found: 73.31% C, 4.25% H, 16.81% N. ^{1}H NMR in $CDCl_3$ (in ppm) 10.4 (s, 2H), 9.45 (d, 4H), 9−9.1 (m, 8H), 8.25 (d, 4H). MALDI MS: $m/z = 464$.

H_2D2n (5,15-Di(pyrid-2-yl)porphyrin): The preparation of H_2-D2n was similar with replacement of pyridine-4-carbaldehyde by pyridine-2-carbaldehyde. An added purification step involved recrystallization from methanol and dichloromethane (8:1 v/v). Calcd for $C_{30}H_{20}N_6 \cdot 0.2CH_2Cl_2$: 74.27% C, 4.17% H, 17.21% N. Found: 74.06% C, 4.32% H, 16.92% N. ^{1}H NMR in $CDCl_3$ (in ppm) 10.4 (s, 2H), 9.46 (d, 4H), 9.24 (d, 2H), 9.16 (d, 4H), 8.36 (d, 2H), 8.20 (td, 2H), 7.79 (td, 2H), −3.10 (broad, 2H). ESI MS: $(m + 1)/z = 465.5$.

[5,15-Di(*N*-methylpyrid-4-yl)porphyrin][tosylate]$_2 \cdot CH_3OH$: Treatment of H_2D4n with methyl tosylate gave the H_2D4 dication, 5,-15-di(*N*-methylpyridinium-4-yl)porphryin. The procedure involved refluxing a solution of H_2D4n and a large excess of methyl tosylate in chloroform.[33,34] A thin-layer analysis showed that one product formed.[35] Separation of the product is straightforward via extraction into water. After evaporation of the water, the final purification step, slow evaporation of a 3:2 mixture of methanol and propanol, yielded blue-purple crystals of the desired product as determined by an X-ray crystallographic analysis.[36]

[5,15-Di(*N*-methylpyrid-2-yl)porphyrin][BF_4]$_2 \cdot 2H_2O$: In accordance with literature methods,[37,38] methylation of H_2D2n occurs in trimethyl phosphate upon exposure to excess methyl triflate at 60 °C. A TLC analysis revealed the formation of one reaction product.[35] After extraction into water, treatment with aqueous BF_4^- yielded a precipitate. Recrystallization from propanol gave the desired product. Calcd for $C_{32}H_{26}N_6O \cdot 2H_2O$: 54.58% C, 4.29% H, 11.93% N. Found: 54.49% C, 4.02% H, 11.97% N. MALDI MS: $m/z = 494$.

Methods. Siliconization of glassware helped minimize absorption of the cationic porphyrins.[39] Commercially obtained oligonucleotides came with the terminal trityl group still attached to allow a purification step on a Poly-Pak column according to the manufacturer's instructions. The purification method for salmon testes (ST) DNA was from the literature.[39]

The extinction coefficients used for concentration determinations were $\epsilon_{260} = 13\,600\ M^{-1}\ cm^{-1}$ for [poly(dA−dT)]$_2$,[40] $\epsilon_{254} = 16\,800\ M^{-1}\ cm^{-1}$ for [poly(dG−dC)]$_2$,[41] and $\epsilon_{260} = 13\,200\ M^{-1}\ cm^{-1}$ for ST DNA, all in units of base pairs.[42] On an oligonucleotide basis, the extinction coefficients were $\epsilon_{260} = 135\,000\ M^{-1}\ cm^{-1}$ for CG-[T4], $\epsilon_{260} = 150\,000\ M^{-1}\ cm^{-1}$ for TT[T4], and $\epsilon_{260} = 142\,000\ M^{-1}\ cm^{-1}$ for TA[T4].[43] The commercial supplier provided the value of $180\,700\ M^{-1}\ cm^{-1}$ for CGCG[T4]. Beer's law plots yielded $\epsilon_{408} = 160\,000\ M^{-1}\ cm^{-1}$ for H_2D4 and $\epsilon_{400.5} = 195\,000\ M^{-1}\ cm^{-1}$ for H_2D2. The absorbance measured after reaction of a solution of H_2D4 with a slight excess of Zn(II) provided a value of $\epsilon_{420} = 155\,000\ M^{-1}\ cm^{-1}$ for Zn(D4). A similar procedure gave $\epsilon_{414} = 183\,000\ M^{-1}\ cm^{-1}$ for Zn(D3).

(27) Littler, B. J.; Miller, M. A.; Hung, C. H.; Wagner, R. W.; O'Shea, D. F.; Boyle, P. D.; Lindsey, J. S. *J. Org. Chem.* **1999**, *64*, 1391−1396.
(28) Wang, Q. M.; Bruce, D. W. *Synlett* **1995**, 1267−1268.
(29) Adler, A. D. *J. Org. Chem.* **1967**, *32*, 476−477.
(30) Manka, J. S.; Lawrence, D. S. *Tetrahedron Lett.* **1989**, *30*, 6989−6992.
(31) Johnstone, R. A. W.; Nunes, M.; Pereira, M. M.; Gonsalves, A.; Serra, A. C. *Heterocycles* **1996**, *43*, 1423−1437.
(32) Chauhan, S. M. S.; Sahoo, B. B.; Srinivas, K. A. *Synth. Commun.* **2001**, *31*, 33−37.
(33) Pasternack, R. F.; Huber, P. R.; Boyd, P.; G., E.; Francesconi, L.; Gibbs, E.; Fasella, P.; Cerio Venturo, G.; deC. Hinds, L. *J. Am. Chem. Soc.* **1972**, *94*, 4511−4517.
(34) Hambright, P.; Gore, T.; Burton, M. *Inorg. Chem.* **1976**, *15*, 2314−2315.
(35) Batinic-Haberle, I.; Spasojevic, I.; Hambright, P.; Benov, L.; Crumbliss, A. L.; Fridovich, I. *Inorg. Chem.* **1999**, *38*, 4011−4022.
(36) Bejune, S. A. Ph.D. Thesis, Purdue University, 2002.
(37) Kaufmann, T.; Shamsai, B.; Lu, R. S.; Bau, R.; Miskelly, G. M. *Inorg. Chem.* **1995**, *34*, 5073−5079.
(38) Miskelly, G. M.; Webley, W. S.; Clark, C. R.; Buckingham, D. A. *Inorg. Chem.* **1988**, *27*, 3773−3781.
(39) Sambrook, J.; Fritsch, J.; Maniatis, T. *Molecular Cloning: A Laboratory Manual*, 2nd ed.; Cold Spring Harbor Laboratory Press: Plainview, NY, 1989.
(40) Inman, R. B.; Baldwin, R. L. *J. Mol. Biol.* **1962**, *5*, 172−184.
(41) Wells, R. D.; Larson, J. E.; Grant, R. C.; Shortle, B. E.; Cantor, C. R. *J. Mol. Biol.* **1970**, *54*, 465−497.
(42) Felsenfeld, G.; Hirschman, S. Z. *J. Mol. Biol.* **1965**, *13*, 407−427.
(43) Lugo-Ponce, P.; McMillin, D. R. *Coord. Chem. Rev.* **2000**, *208*, 169−191.

For the DNA binding studies the buffer was a $\mu = 0.1$, pH 6.8 phosphate buffer that included 0.05 M NaCl. The porphyrin concentration was 1.7 μM for all spectrophotometric work. To compensate for any offset, the baseline adjustment is such that each CD spectrum goes through zero at 480 nm. The calculated %*H*, or hypochromic response, represents the percent drop in absorbance at the Soret maximum due to adduct formation with DNA. During luminescence measurements, long wave pass filters facilitated isolation of the emission from the excitation light, and the bandpass was 5 nm for both excitation and emission. The correction for the influence of absorbance on the emission intensity was eq 1, where I represents the experimental emission intensity, I_c is the corrected emission intensity, and A is the absorbance at the excitation wavelength.

$$I_c = \frac{I}{1 - 10^{-A}} \quad (1)$$

For viscometry studies, solutions contained ST DNA at a concentration of 70 μM in base pairs. After sonication, the mean length of the DNA molecules was about 500 base pairs as established by gel electrophoresis. The calculated standard reduced viscosity (SRV) ratio comes from eq 2.

$$\frac{\eta}{\eta_0} = \frac{t_c - t_0}{t_D - t_0} \quad (2)$$

where t_0 is the flow time of the buffer, t_D is the flow time of DNA in buffer, and t_c is the flow time of the DNA solution containing porphyrin. For each measurement at 25 °C, the average of the first three consecutive runs that agreed with each other to within ± 1 s defined the flow time. The buffer was a $\mu = 0.01$ M Tris solution at pH 7.5.

The method of Kelly and Murphy was useful for the gel studies with pBR322 plasmid DNA and topoisomerase I.[44] In brief, the preparatory phase involved incubation of 0.12 nmol of plasmid base pairs with 10 units of topoisomerase I in 50 μL of reaction buffer (50 μM Tris, 50 mM KCl, 10 mM $MgCl_2$, 0.5 mM DTT, 0.1 mM EDTA, 30 μg/mL bovine serum albumin) for 1 h at room temperature. Step 2 was addition of porphyrin and incubation for another 1.5 h. Treatment with a phenol:chloroform:isoamyl alcohol mixture (25:24:1) containing 0.5% (w/v) 8-hydroxyquinoline quenched the reaction and yielded the plasmid in the aqueous layer. The final preparation steps were precipitation of the DNA with cold ethanol and dissolution in buffer. The electrophoresis was for 6 h in a 40 V applied field. Treatment with ethidium bromide permitted visualization of the DNA in the gel.

Instrumentation. A Varian Cary 100 Bio UV−visible spectrophotometer provided all absorbance data. The fluorescence spectrophotometer was a Varian Cary Elipse, complete with an R3896 phototube, and the circular dichroism (CD) spectropolarimeter was a JASCO Model J810. The NMR spectrometer was a Gemini-Varian 200 or an Inova 300 MHz unit. The viscometer was a Cannon-Ubbelohde Model 50 or a Cannon-Manning Model 25. Immersion in a standard water bath provided a constant-temperature environment. Other routine equipment used included a Corning Model 430 pH meter, a Branson W-350 sonifier, a Kenmore microwave oven, and a Sevant Instruments Model CVR300 power supply for electrophoresis.

Results

New Dipyridyl Porphyrins. In 5,15-di(pyrid-4-yl)porphyrin (H_2D4n), pyridines bind via their C4 atoms to alternate meso carbons of the macrocyclic ring system, whereas in the 5,15-di(pyrid-2-yl)porphyrin (H_2D2n) isomer, the links are to the C2 carbons. Absorption data for the two neutral porphyrin derivatives as well as the other linkage isomer H_2D3n, or 5,15-di(pyrid-3-yl)porphyrin, appear in Table 1. The table also includes data for the dicationic forms H_2D4 = 5,15-di(*N*-methylpyridinium-4-yl)porphyrin, H_2D2 = 5,15-di(*N*-methylpyridinium-2-yl)porphyrin, and H_2D3 = 5,15-di(*N*-methylpyridinium-3-yl)porphyrin in aqueous buffer solution. Figure 1 displays the absorption spectrum of H_2D4 and the zinc(II) adduct Zn(D4). See Table 1 for peak maxima.

Table 1. Absorbance Data for Dipyridyl Porphyrins

porphyrin	absorption maxima,[a,b] nm
H_2D4n	405, 500, 537, 574, 629
H_2D2n	406, 502, 535, 574, 628
H_2D3n	405, 500, 533, 575, 633
H_2D4	408 [160], 505, 547, 570sh, 624
H_2D2	401 [195], 501, 537, 567, 620
H_2D3	403 [200], 502, 538, 565, 617
Zn(D4)	420 [155], 545, 592
Zn(D3)	414 [183], 544, 581

[a] In dichloromethane for neutral porphyrins and in $\mu = 0.1$, pH 6.8 phosphate buffer for cationic forms. [b] Molar extinction coefficients in square brackets (mM^{-1} cm^{-1}).

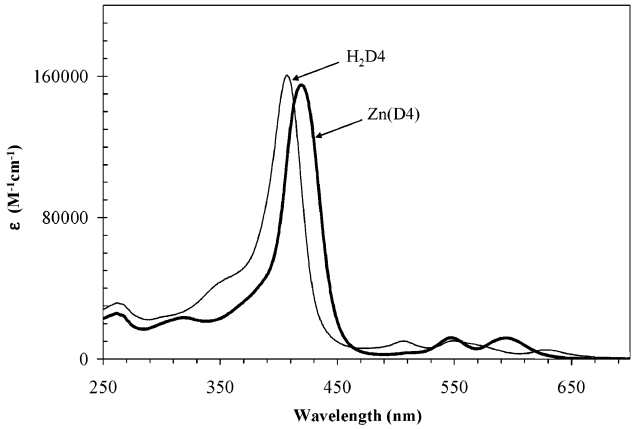

Figure 1. Absorption spectra of H_2D4 and Zn(D4) (thick line) in $\mu = 0.1$ M phosphate at pH 6.8.

Spectral studies of H_2D2 and H_2D4 with DNA Polymers. Figure 2 shows how the Soret band of H_2D2 responds to the addition of $[poly(dG-dC)]_2$. By a DNA base pair to porphyrin (bp/p) ratio of 50:1, the red shift in the Soret band reaches a maximum of about 19 nm. The hypochromic effect (*H*) is 54% as measured by the comparison of absorbance maxima; however, the decrease in absorbance intensity is partly due to an increase in the bandwidth for the DNA-bound form. As is evident from the data in Table 2, the corresponding spectral changes are smaller for adduct formation between H_2D2 and $[poly(dA-dT)]_2$. For interaction between H_2D4 and excess $[poly(dG-dC)]_2$, the bathochromic shift is 27 nm, and the hypochromic effect is 40% (Figure 3). With H_2D4 the binding is more efficient by comparison with H_2D2 because there is no sign of any unbound porphyrin even at bp/p = 5. However, no isosbestic point occurs in Figure 3 during DNA addition. Along with the shifting trend in hypochromism, this suggests that more

(44) Kelly, J. M.; Murphy, M. J.; McConnell, D. J.; Ohuigin, C. *Nucleic Acids Res.* **1985**, *13*, 167−184.

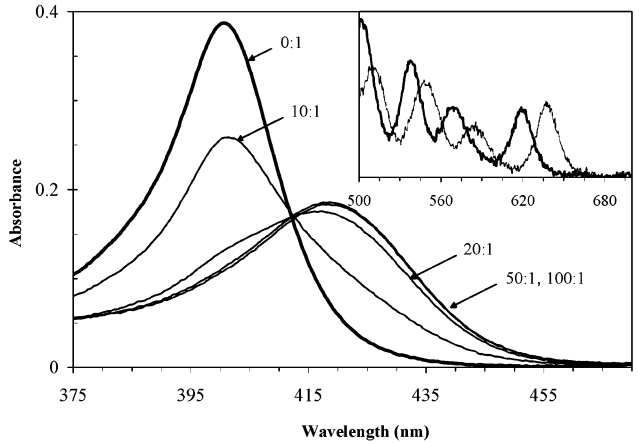

Figure 2. Absorption of H_2D2 in the presence of varying amounts of $[poly(dG-dC)]_2$ in the same buffer as Figure 1. The labels are the bp/p ratios. Inset: Q-band absorption of free H_2D2 (thick line) and the adduct with bp/p = 100:1.

Table 2. Physical Data for Dipyridyl Porphyrins with DNA in $\mu = 0.1$ M, pH 6.8 Phosphate

		Soret		CD		emission
DNA	porphyrin	$\Delta\lambda$, nm	% H	λ, nm	$\Delta\epsilon$, M^{-1} cm^{-1}	λ, nm
$[poly(dG-dC)]_2$	H_2D4	27	42	428	−3	662, 722
	H_2D2	19	50	450	−4	643, 209
	H_2D3[a]	20	36	420br	−3	
	Zn(D4)	15	39	436	−3	630
	Zn(D3)[a]	12	26	416	−3	
$[poly(dA-dT)]_2$	H_2D4	22	28	427	−20	653, 715
	H_2D2	16	21	412	−4	638, 703
				430	4	
	H_2D3[a]	16	24	417	−25	
	Zn(D4)	12	26	431	−16	620
	Zn(D3)[a]	4	26	415	−15	
ST	H_2D4	21	27	417	−2	657, 720
	Zn(D4)	13	16	423	−8	628
CG[T4]	H_2D4	23	37	422	−10	653, 714
	H_2D3[a]	19	44	417	−10	
TT[T4]	H_2D4	21	27	423	−17	651, 712
	H_2D3[a]	17	29	417	−18	
TA[T4]	H_2D4	21	23	426	−17	653, 714
CCGG[T4]	H_2D4	22	30	426	−10	654, 716

[a] Reference 26.

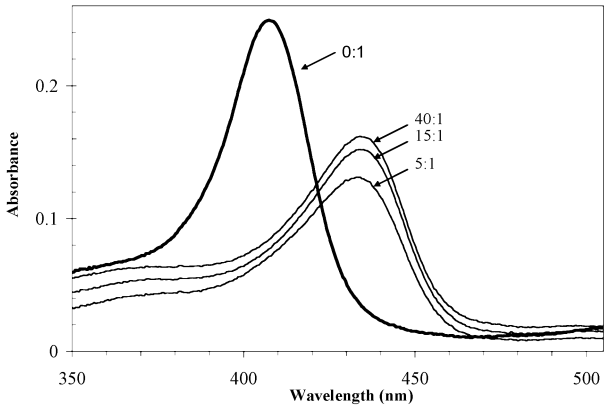

Figure 3. Absorption of H_2D4 in the presence of varying amounts of $[poly(dG-dC)]_2$ in the same buffer as Figure 1. The labels are the bp/p ratios.

than one type of adduct forms during the titration. Similar anomalies occur in the longer wavelength, so-called Q-band region. (See below for a description of analogous results obtained with the CCGG hairpin.) Adduct formation between

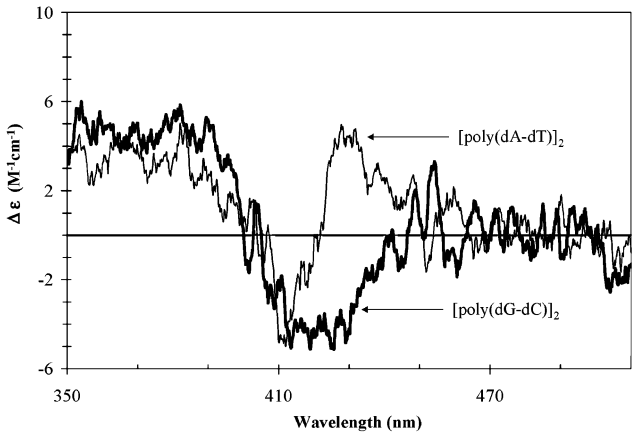

Figure 4. Circular dichroic (CD) spectra of H_2D2 bound to $[poly(dG-dC)]_2$ (thick line) and $[poly(dA-dT)]_2$ in the same buffer as Figure 1 at bp/p = 100:1.

H_2D4 and $[poly(dA-dT)]_2$ also induces significant shifts ($\Delta\lambda$ = 22 nm and H = 28%) in the Soret region. However, both shifts are smaller for the corresponding adduct of H_2D2.

Bathochromic shifts observed in emission spectra parallel those in the absorbance data. For free H_2D4 the emission spectrum consists of the zero−zero band, which connects the ground vibrational levels of the two electronic states involved, at 635 nm and a weaker band at 697 nm. Corresponding maxima occur at 626 and 685 nm in the emission spectrum of H_2D2. On binding to DNA both emission spectra exhibit shifts toward longer wavelength, but the shift is larger with H_2D4. In the presence of excess $[poly(dG-dC)]_2$, the zero−zero band of H_2D4 shifts 28 nm versus 16 nm for H_2D2. There is no change in intensity for the H_2D4 system; however, the emission intensity from H_2D2 decreases by 50%. With $[poly(dA-dT)]_2$ the corresponding shifts are 17 nm for H_2D4 and 12 nm for H_2D2. The emission intensity of H_2D4 increases almost 60%, but there is no change with H_2D2.

In the presence of an excess of either DNA polymer, H_2D4 shows a negative induced circular dichroism (CD) signal in the Soret region. The signal of the adduct with $[poly(dA-dT)]_2$ centers about 427 nm, where $\Delta\epsilon = -20$ M^{-1} cm^{-1}. With $[poly(dG-dC)]_2$ the adduct gives a weaker signal ($\Delta\epsilon = -4$ M^{-1} cm^{-1}) centered around 430 nm. Figure 4 shows that the adduct of H_2D2 with $[poly(dG-dC)]_2$ also exhibits a negative CD signal; however, interaction with $[poly(dA-dT)]_2$ induces a derivative-like signal. In line with absorbance data, the CD spectra center around 420 nm (Figure 4).

Spectral studies of H_2D4 with DNA Hairpins. The spectral data in Table 2 for adducts of H_2D4 with the TA[T4], TT[T4], and CG[T4] hairpins correlate nicely with the results for the polymer systems. Comparison of absorption spectra for H_2D4 at hairpin-to-porphyrin (hp/p) ratios of 5:1 and 10:1 reveal that adduct formation is complete at the 5:1 ratio. In the Soret region, the bathochromic shift is 21 nm for adduct formation with the TA[T4] or TT[T4] hairpin versus 23 nm with the CG[T4] hairpin. The emission spectra of the adducts all shift to longer wavelength, the smallest shift occurring with the adduct of the TT[T4] hairpin. For

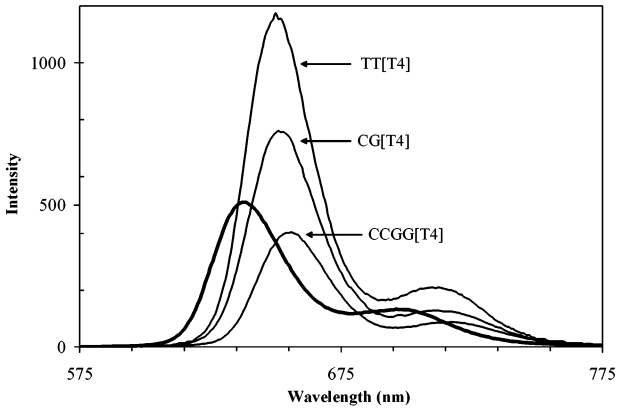

Figure 5. Emission spectra of H_2D4 in the free state (thick line) and bound to three different hairpins, buffered as before. Areas reflect relative intensities, and hp/p = 5:1 except for CCGG[T4], where hp/p = 15:1.

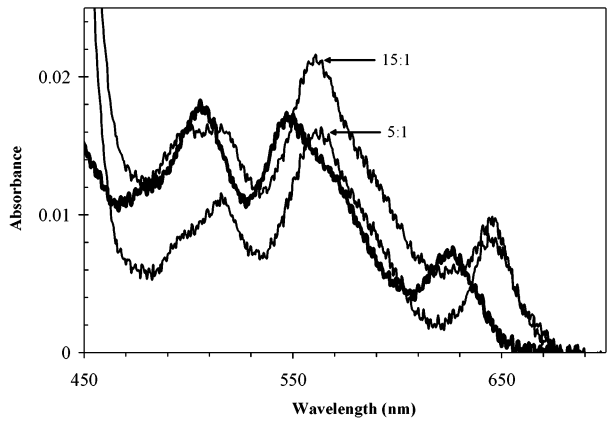

Figure 6. Absorption of H_2D4 in the Q-band region as a function of the concentration of CCGG[T4]. The hp/p ratio is 0:1 (thick line), 5:1, or 15:1. Buffered as in Figure 1.

all three 16-mers, adduct formation leads to approximately a 2-fold increase in emission intensity (Figure 5). The induced CD signal is negative in every case and the least intense in the case of the CG hairpin (Table 2). The interaction of H_2D4 with the long-stem hairpin CCGG[T4] shows some of the same complications noted earlier for adduct formation with $[poly(dG-dC)]_2$. With the CCGG-[T4] hairpin the net spectral shifts, induced CD intensity, and degree of hypochromism compare favorably with those of the other hairpin adducts (Table 2). However, adduct formation is not complete until a hairpin-to-porphyrin ratio of 10:1, and there is no isosbestic point in the absorption spectrum during addition of the long-stem hairpin.

Figure 6 reveals noteworthy spectral changes that occur in the Q-band region as a result of interaction with CCGG-[T4]: (1) As with the $[poly(dG-dC)]_2$ system, the hypochromism is maximum when low levels of DNA are present. (2) Another parallel with the $[poly(dG-dC)]_2$ system is that adduct formation induces a *hyperchromic* effect in the zero−zero bands, here at around 550 and 640 nm. (3) Finally, the absorption at ca. 500 nm appears to consist of two overlapping transitions. One other intriguing observation is that the adduct with the CCGG[T4] hairpin is the only bound form of H_2D4 to show partial quenching of the emission (Figure 5).

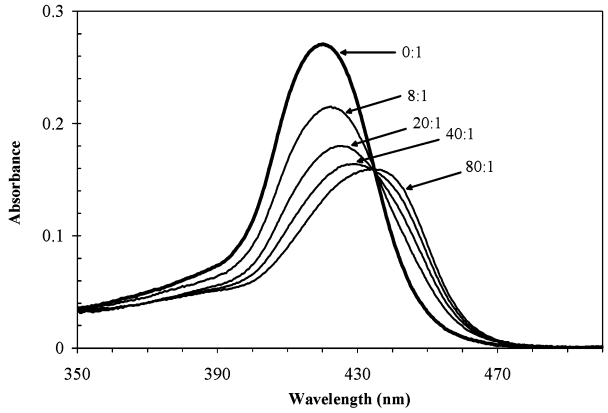

Figure 7. Absorption of Zn(D4) in the presence of varying amounts of $[poly(dG-dC)]_2$. The labels designate bp/p ratios. Buffered as in Figure 1.

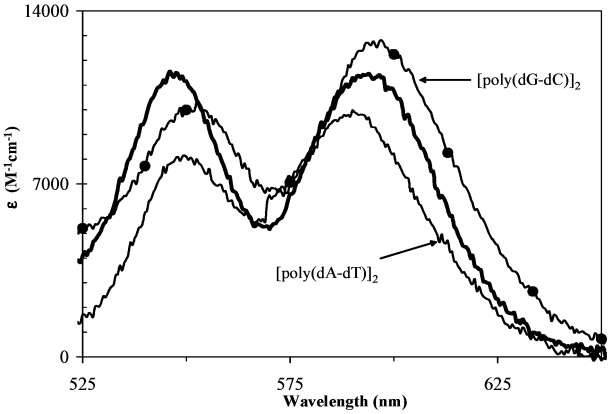

Figure 8. Absorption spectra of Zn(D4) in the Q-band region. Free porphyrin (thick line); adduct with $[poly(dG-dC)]_2$ (− · −); and adduct with $[poly(dA-dT)]_2$ (—). Buffered as in Figure 1 with bp/p = 80:1.

Spectral Studies of Zn(D4) with DNA Polymers. The adducts formed by Zn(D4) exhibit very different spectral properties. Figure 7 shows how the Soret band of Zn(D4) responds to the addition of $[poly(dG-dC)]_2$. Although adduct formation induces a significant hypochromic response ($H \approx$ 39%), the bathochromic shift of $\Delta\lambda \approx 17$ nm is comparatively modest. Moreover, uptake is not complete until the bp/p ratio is of the order of 80:1, compared with 40:1 for H_2D4. Table 2 shows that the spectral shifts are even smaller for the other adducts of Zn(D4). Figure 8 provides a comparison of spectra for the various adducts in the Q-band region.

Another contrast with the H_2D4 system is that the emission spectrum of Zn(D4) lacks resolved vibronic structure. See Figure 9 and Table 2 for a summary of the data. Upon interaction with $[poly(dA-dT)]_2$, the emission increases, but adduct formation with $[poly(dG-dC)]_2$ or ST DNA leads to partial quenching. In each case the shift in emission wavelength is small. The adduct with $[poly(dA-dT)]_2$ is remarkable in that the spectral shift is toward shorter wavelength.

The adduct with $[poly(dA-dT)]_2$ is also notable in that it has the strongest CD signal in the Soret region (Figure 10 and Table 2). The signal is relatively sharp and has a maximum amplitude of $-16\ M^{-1}\ cm^{-1}$. The adduct with $[poly(dG-dC)]_2$ also gives a negative signal, but with a

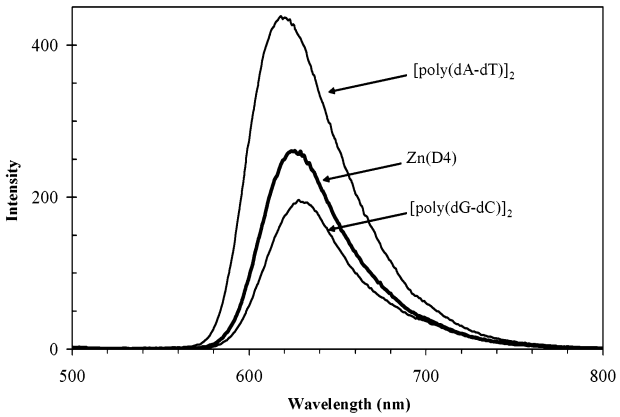

Figure 9. Emission from free Zn(D4) (thick line) and adducts with [poly(dG−dC)]$_2$ and [poly(dA−dT)]$_2$ at bp/p = 80:1. The results with ST DNA closely track those obtained with [poly(dG−dC)]$_2$. Areas reflect relative intensities. Same buffer as in Figure 1.

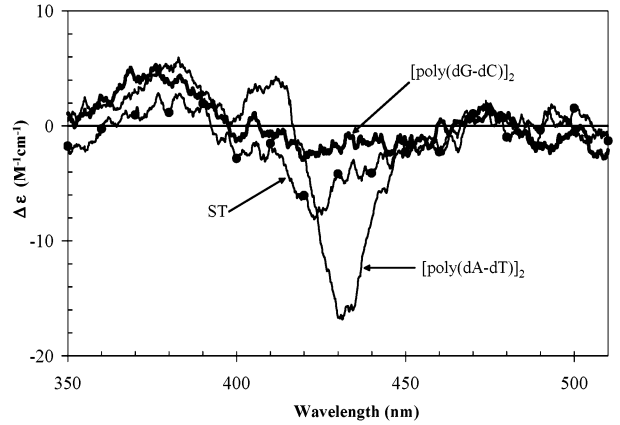

Figure 10. CD spectra of Zn(D4): with [poly(dG−dC)]$_2$ at bp/p = 40:1 (thick line), with [poly(dA−dT)]$_2$ at bp/p = 15:1 (—), and with ST DNA at bp/p = 80:1 (— · —). Buffered as in Figure 1.

weaker amplitude and a broader bandwidth. Adduct formation with random-sequence ST DNA seems to give rise to a composite CD signal. More specifically, there is a relatively sharp CD signal at around 425 nm that rests on top of a broader, underlying signal (Figure 10).

Mobility Studies. Changes in flow properties occur if porphyrin uptake affects the shape, length, and/or rigidity of the DNA host. Plots in Figure 11 reveal how the reduced viscosity ratio of ST DNA varies with loading of different porphyrins. Previous reports show that the specific viscosity of DNA decreases upon uptake of the bulky Zn(T4) system.[45] In accordance with those findings, Figure 11 shows that the η/η_0 ratio decreases with addition of Zn(T4), i.e., as the porphyrin-to-base-pair (p/bp) ratio increases. In contrast, the specific viscosity of the DNA nearly doubles with the loading of Zn(D3) or H_2D4.

Gel mobility studies with covalently closed supercoiled (CCS) DNA molecules provide complementary information. During electrophoresis, commercially available pBR322 DNA separates into a slow-moving nicked form and the comparatively mobile CCS form. After incubation with

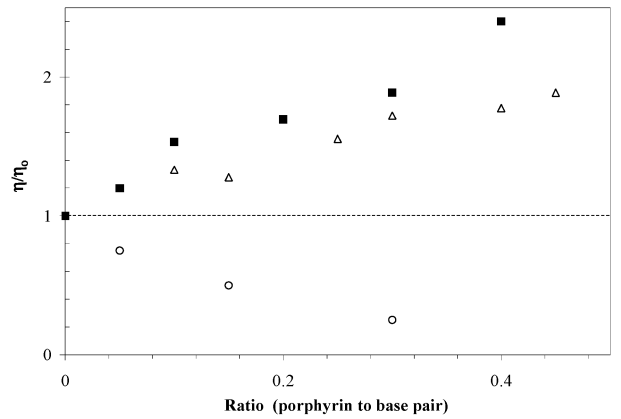

Figure 11. Standard viscosity ratio of ST DNA in the presence of Zn(T4) (○); Zn(D3) (△), or H_2D4 (■). The DNA concentration is 70 μM in base pairs in μ = 0.01 M Tris at pH 7.9. Zn(D3) data described in part in ref 26.

topoisomerase I, a series of bands representing partially relaxed forms of intermediate mobility appear in lieu of the CCS component. After addition of Zn(D3), continued incubation leads to recovery of the CCS form, but the addition of Zn(T4) has no effect.

Discussion

Porphyrin Synthesis. The acetic or propionic acid solvent system for porphyrin synthesis is similar to the one introduced by Adler.[29] In modern syntheses of porphyrins, the reaction medium is often dichloromethane in combination with a catalytic amount of a strong acid; however, these conditions are often ineffective with heteroaromatic aldehydes.[46,47] The 2−4% isolated yields of the *trans*-dipyridylporphyrins reported herein are meager but are superior to those obtained in early attempts with the other solvent system. The main porphyrin byproduct is the monopyridylporphyin. Substituent scrambling is possible if intermediates form reversibly.[48,49] Here, decomposition of dipyrromethane with release of pyrrole would provide the ingredients for formation of monopyridylporphyrin. However, in the very large number of syntheses carried out during the developing stages of this study, there was never any sign of another likely byproduct of scrambling, namely *cis*-dipyridylporphyrin.

Intercalation of H_2D4. Unlike the often-studied tetrapyridyl H_2T4 ligand, physical data leave little doubt but that H_2D4 intercalates into double-stranded, B-form DNA regardless of the nature of the base pairs. The same is true of H_2-D3.[26] Uptake of H_2D4 by either [poly(dG−dC)]$_2$ or [poly(dA−dT)]$_2$ induces bathochromic (27 vs 22 nm) and hypochromic (42 vs 28%) shifts that are indicative of strong coupling to the π system of the H_2D4 chromophore. The spectral perturbations would be smaller for external, or

(45) Banville, D. L.; Marzilli, L. G.; Wilson, W. D. *Biochem. Biophys. Res. Commun.* **1983**, *113*, 148−154.

(46) Drain, C. M.; Gong, X. C.; Ruta, V.; Soll, C. E.; Chicoineau, P. F. *J. Comb. Chem.* **1999**, *1*, 286−290.
(47) Gryko, D.; Lindsey, J. S. *J. Org. Chem.* **2000**, *65*, 2249−2252.
(48) Littler, B. J.; Ciringh, Y.; Lindsey, J. S. *J. Org. Chem.* **1999**, *64*, 2864−2872.
(49) Hombrecher, H. K.; Horter, G.; Arp, C. *Tetrahedron* **1992**, *48*, 9451−9460.

groove, binding because of the less direct contact between π systems.[2−5] The fact that both H_2D4 adducts exhibit negative induced CD signals in the Soret region is also a sign of intercalation and is incompatible with groove binding which normally induces a positive response.[17] In accordance with results obtained with H_2D3, the adduct of H_2D4 with $[poly(dG-dC)]_2$ exhibits a weak CD signal. The CD signal and the Soret absorption band are also broad by comparison with those of the $[poly(dA-dT)]_2$ analogue. One explanation for the bandwidth could be that the 5′-CpG-3′ and 5′-GpC-3′ steps of $[poly(dG-dC)]_2$ both support intercalation and that the two signals are different enough to broaden the envelope.

Viscometry data provide final confirmation that intercalation is the preferred mode of binding for H_2D4. For moderate chain lengths, intercalation of a substrate into a B-form double helix tends to increase the length and rigidity of the helix, and both factors enhance the DNA contribution to the solution viscosity.[50,51] Consistent with intercalative binding, Figure 11 shows that the uptake of H_2D4 enhances the standard reduced viscosity (SRV) ratio. Note that uptake of Zn(T4), which binds externally to DNA,[17,45] induces a *decrease* in the SRV.

Concentration Dependence of H_2D4 Binding. Although the principal mode of interaction between H_2D4 and $[poly(dG-dC)]_2$ is evident, the lack of an isosbestic point in the absorption spectrum during the addition of the DNA shows that the interaction is more complicated than simple 1:1 adduct formation. In addition, the data in Figure 3 show that the hypochromism maximizes at high loadings of porphyrin, when H_2D4 is in excess. One possible explanation is that the porphyrin aggregates on the DNA substrate at the higher porphyrin-to-base-pair ratios. However, so-called outside stacking of the porphyrin normally gives rise to porphyrin/porphyrin interactions that induce a conservative, or bisignate, CD signal that can be quite intense.[52,53] Here, the induced CD signal remains weak, negative, and strictly monosignate throughout the titration. An alternative explanation for the absorbance changes is cooperative binding of H_2D4 to $[poly(dG-dC)]_2$. Cooperative interactions occur when intercalation of one porphyrin affects the binding and the spectral properties of a second porphyrin molecule, usually bound nearby. Such effects are likely when porphyrin molecules cluster near one another at the early stages of DNA addition. When the host is in large excess, the ligands are free to disperse to essentially independent intercalation sites. There are many precedents for cooperative binding to DNA in the literature. The ligands involved range from metal polypyridine complexes, which act as partial intercalators,[54,55] to groove-binding systems such as netropsin.[56]

Spectral differences in the cooperatively bound form may reflect porphyrin/porphyrin interactions, site-to-site differences in the local rigidity of the double helix, and/or variations in the twist angle the porphyrin adopts relative to the adjacent base pairs. However, absorbance data in the Q-band region suggest another intriguing possibility. As in Figure 6, interaction with $[poly(dG-dC)]_2$ induces a bathochromic shift in the Q-bands of H_2D4, but there is a definite *hyperchromic* effect. In the absence of higher order effects, simple excitonic coupling with transitions of the DNA bases would give rise to a hypochromic response. This effect not withstanding, the variation in absorption intensity is easy to understand if the dihedral angle subtended by the pyridinium substituents changes with dispersement of the porphyrin. More specifically, the prediction is that the pyridinium groups rotate more nearly into the plane of the porphyrin core as the average distance between porphyrins increases. The resulting increase in conjugation would lead to an increase in absorption intensity as well as a shift to lower energy. Observations involving the H_2D3 and H_2D2 porphyrins are consistent with this reasoning. Thus, adduct formation between H_2D3 and $[poly(dG-dC)]_2$ or $[poly(dA-dT)]_2$ induces the same type of hyperchromism in the Q-band region.[57] On the other hand, hyperchromism is much less apparent in Figure 2, perhaps because the *o*-methyl groups of the pyridine substituents in H_2D2 severely constrain the range of dihedral angles available.

Adducts with DNA Hairpins. The H_2D4 porphyrin also binds by intercalation into the DNA hairpins investigated. Hairpins are useful substrates because the stems retain a duplex structure even at very low oligonucleotide concentrations, base replacement is straightforward, and competitive binding studies are feasible.[16,25,43] The three 16-mers used here differ only by the bases present in positions 3 and 4 and the complementary positions 14 and 13, respectively. For example, in the XY[T4] structure shown, X = T, X′ = A, Y = A, and Y′ = T for the TA[T4] hairpin. Hairpins of

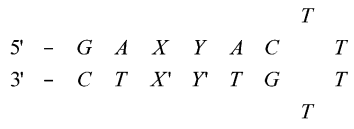

XY[T4]

this type have a tight loop structure,[58] and all evidence to date suggests that they take up porphyrin exclusively in the stem regions.[43] Since the stems of the TA[T4] and TT[T4] hairpins are rich in A=T base pairs, it is not surprising that their adducts with H_2D4 exhibit CD and absorption spectra very similar to those of the $[poly(dA-dT)]_2$ adduct. One interesting observation is that the amplitude of the induced CD signal for the CG[T4] adduct is about double that of the $[poly(dG-dC)]_2$ adduct. The local conformation of the DNA

(50) Muller, W.; Crothers, D. M. *J. Mol. Biol.* **1968**, *35*, 251−290.
(51) Banville, D. L.; Marzilli, L. G.; Strickland, J. A.; Wilson, W. D. *Biopolymers* **1986**, *25*, 1837−1858.
(52) Carvlin, M. J.; Dattagupta, N.; Fiel, R. J. *Biochem. Biophys. Res. Commun.* **1982**, *108*, 66−73.
(53) Pasternack, R. F.; Brigandi, R. A.; Abrams, M. J.; Williams, A. P.; Gibbs, E. J. *Inorg. Chem.* **1990**, *29*, 4483−4486.
(54) Lincoln, P.; Tuite, E.; Norden, B. *J. Am. Chem. Soc.* **1997**, *119*, 1454−1455.
(55) Olson, E. J. C.; Hu, D. H.; Hormann, A.; Barbara, P. F. *J. Phys. Chem. B* **1997**, *101*, 299−303.
(56) Wemmer, D. E. *Biopolymers* **1999**, *52*, 197−211.
(57) Wall, R. K. M.S. Thesis, Purdue University, 2001.
(58) van Dongen, M. J. P.; Mooren, M. M. W.; Willems, E. F. A.; van der Marel, G. A.; van Boom, J. H.; Wijmenga, S. S.; Hilbers, C. W. *Nucleic Acids Res.* **1997**, *25*, 1537−1547.

may differ in the more flexibile hairpin structure. The CCGG-[T4] hairpin is related to CG[T4], except the stem contains two more C≡G base pairs. Here, the elongated stem seems to promote the same type of cooperative binding noted earlier for the $[poly(dG-dC)]_2$ system. Thus, the Q-band absorption depicted in Figure 6 shows evidence of hypochromism at a hairpin-to-porphyrin ratio of 5:1, but with larger excesses of hairpin, the response becomes essentially hyperchromic. A hairpin-to-porphyrin ratio of about 10:1 is necessary to ensure that no hairpin binds more than one porphyrin.

Another interesting aspect of Figure 6 is the structure associated with the absorption that occurs around 500 nm. In principle, the short-wavelength shoulder could represent a vibronic transition involving a high frequency combination band of the porphyrin excited state. Alternatively, the spectrum may reflect binding in two different step types as discussed above. Still another possibility is that one of the bands represents a charge-transfer absorption involving H_2-D4 and one of the bases of the DNA host.

Influence on the Emission from H_2D4. In most cases, even adduct formation with $[poly(dG-dC)]_2$, intercalation into DNA does not lead to a quenching of the emission from H_2D4. This contrasts with the results obtained with the tetrapyridyl analogue H_2T4, where intercalation between G≡C base pairs leads to a diminution of emission from the porphyrin.[44] One explanation is electron-transfer quenching, but recent work argues that charge-transfer complex formation between the excited state and a guanine residue is more likely.[16] Either way, the reducing character of guanine promotes quenching. Since H_2D4 is only a dication, the excited state will not be as potent an electron acceptor, and guanine will not be as effective a quencher. The one substrate that does induce weak quenching is the CCGG[T4] hairpin. This result is intriguing because a stacked pair of guanines is more reducing than a single guanine residue.[59−61] A likely interpretation of the quenching results is that H_2D4 intercalates next to at least one of the 5′-GpG-3′ steps in the stem of the CCGG[T4] hairpin.

Zinc(II) Porphyrins. The zinc(II) forms of the dipyridylporphyrins H_2D3 and H_2D4 provide interesting test cases because Zn(T4) almost exclusively binds externally to DNA. The accepted explanation relies on crystallographic studies which have established that Zn(T4) is five coordinate.[62] The argument is that with even one axial ligand the porphyrin is simply too thick to intercalate into B-form DNA.[17] However, even though the zinc(II) ion is a bit large for the porphyrin cavity, there are other structurally characterized forms in which the zinc center is four coordinate and resides in the plane of the porphyrin.[63] There is also one report that Zn-(T4) can lose the axial water ligand and intercalate into B-form DNA at a sufficiently low ionic strength, despite the steric problems associated with the uptake of a tetrapyridylporphyrin.[64]

Physical studies reveal that Zn(D4) and Zn(D3) intercalate into $[poly(dG-dC)]_2$ as well as $[poly(dA-dT)]_2$, but the results differ in many ways from those obtained with H_2D4. For example, interaction with $[poly(dG-dC)]_2$ induces a relatively modest bathochromic shift in the Soret band of Zn(D4), although there is a significant hypochromic effect (Figure 7 and Table 2). The binding constant is also lower because completion of adduct formation with Zn(D4) requires a 10-fold higher DNA base pair to porphyrin ratio. The emission from Zn(D4) is also distinctive for the lack of vibronic structure and the unusual energy changes. Binding to ST DNA or $[poly(dG-dC)]_2$ induces the emission to shift to a slightly longer wavelength; however, the emission is in the opposite direction for adduct formation with $[poly(dA-dT)]_2$. Zn(D4) evidently does not have much of a base preference because the spectral properties of the ST adduct are intermediate between those of the $[poly(dA-dT)]_2$ and $[poly(dG-dC)]_2$ adducts and only slightly closer to the latter. There is little doubt but that Zn(D4) is an intercalator because the induced CD signal is always negative. The viscosity increases induced in ST DNA by the binding of Zn(D3) or Zn(D4) and the fact that Zn(D3) induces supercoil formation in a circular DNA plasmid completely validate this conclusion. Early on, the Fiel group made similar measurements in their studies involving H_2T4.[65] Although the hypochromic effects, induced CD signals, and mobility data establish the mode of binding, the observed shifts of the absorption and emission maxima of Zn(D4) require further explanation.

The confusion arises because the spectral shifts reflect two opposing trends. One effect is that the zinc center must shed an axial ligand in order to slide into the base stack. Previous work has shown that the absorption bands of zinc porphyrins shift toward *shorter* wavelengths upon loss of an axial ligand.[66,67] At the same time coupling with the π systems of the DNA bases tends to induce a shift in the opposite direction. A similar competition is in effect when the six-coordinate form of Ni(T4) loses two axial water molecules in order to take up an intercalation site in DNA. With Ni-(T4), the net result is a hypochromic shift in the Soret band, instead of the bathochromic shift that intercalators normally exhibit.[17,68]

Two other spectral properties are worth noting. The first is that the adduct of Zn(D4) with $[poly(dG-dC)]_2$ exhibits relatively broad absorption bands in both the Soret and Q-band regions. Vibronically induced broadening can occur if there are intrinsic structural differences between the ground and the excited states. For example, a doming distortion of

(59) Prat, F.; Houk, K. N.; Foote, C. S. *J. Am. Chem. Soc.* **1998**, *120*, 845−846.
(60) Lewis, F. D.; Wu, T. F.; Liu, X. Y.; Letsinger, R. L.; Greenfield, S. R.; Miller, S. E.; Wasielewski, M. R. *J. Am. Chem. Soc.* **2000**, *122*, 2889−2902.
(61) Saito, I.; Nakamura, T.; Nakatani, K. *J. Am. Chem. Soc.* **2000**, *122*, 3001−3006.
(62) Collins, D. M.; Hoard, J. L. *J. Am. Chem. Soc.* **1970**, *92*, 3761−3771.
(63) Scheidt, W. R.; Kastner, M. E.; Hatano, K. *Inorg. Chem.* **1978**, *17*, 706−710.
(64) Chirvony, V. S.; Galievsky, V. A.; Terekhov, S. N.; Dzhagarov, B. M.; Ermolenkov, V. V.; Turpin, P. Y. *Biospectroscopy* **1999**, *5*, 302−312.
(65) Fiel, R. J.; Munson, B. R. *Nucleic Acids Res.* **1980**, *8*, 2835−2842.
(66) Corwin, A. H.; Whitten, D. G.; Baker, E. W.; Kleinspehn, G. G. *J. Am. Chem. Soc.* **1963**, *85*, 3621−3624.
(67) Miller, R. J.; Dorough, D. G. *J. Am. Chem. Soc.* **1952**, *74*, 3977−3981.
(68) Yue, K. T.; Lin, M. F.; Gray, T. A.; Marzilli, L. G. *Inorg. Chem.* **1991**, *30*, 3214−3222.

the porphyrin could occur in the excited state if the zinc center tends to shift out of the plane of the porphyrin. Alternatively, as postulated above for H_2D4, the broadening may simply mean that the chromophore intercalates between both 5′-CpG-3′ and 5′-GpC-3′ steps in the DNA sequence. The other interesting observation is the relatively narrow spacing between Q-bands for the adduct of Zn(D4) with $[poly(dA-dT)]_2$; see Figure 8. This could indicate a significant structural difference within the adduct.

Binding of H_2D2. The rigidity of the H_2D2 and H_2T2 porphyrins can affect binding because the *o*-methyl groups essentially constrain the substituents to be perpendicular to the plane of the porphyrin. In light of the fact that H_2T2 only binds externally to DNA, a common inference is that a porphyrin cannot intercalate unless it has meso substituents that can rotate into the plane of the porphyrin long enough to permit passage between the base pairs.[17,69] Results obtained with the dicationic 5,15-diphenyl-10,20-di(*N*-methylpyridinium-4yl)porphyrin and 5,10-diphenyl-15,20-di(*N*-methylpyridinium-4yl)porphyrin isomers are consistent with the model.[70] Thus, only the isomer with *cis*-phenyl substituents intercalates, ostensibly because it can wedge through the base pairs via the edge that contains the relatively freely rotating phenyl substituents. However, the double helix is constantly opening and closing due to thermal agitation. So-called threading intercalators have bulky ends that inhibit the kinetics of uptake or release, but they do not necessarily destabilize the adduct itself.[71,72] In view of the hypochromic response, the substantial bathochromic shift (19 nm), and the negative induced CD signal observed in the Soret region, the H_2D2 system is also obviously able to intercalate into $[poly(dG-dC)]_2$. Steric inhibition is nonetheless evident because it takes about 10 times as much DNA to drive adduct formation to completion with H_2D2 as compared with H_2D4. The strain probably arises from steric interactions between substituent methyl groups and peripheral atoms of the bases at the top and bottom of the intercalation site. This problem will be even more acute with H_2T2. With a pair of pyridinium-2-yl groups in the minor groove, the intercalated form of H_2T2 would also have to adopt a more or less predetermined twist angle relative to the bases. Strain evidently affects the binding of H_2D2 with $[poly(dA-dT)]_2$ as well, and the nature of the adduct is uncertain. The bathochromic shift and the hypochromic effect in the Soret region are large for external binding, but the CD signal is inconsistent with classical intercalative binding.

Energy Picture

Any analysis of the energetics of adduct formation must include endoergic as well as exoergic factors. Destabilizing factors may include requirements for structural reorganization of the host or the guest as well as any steric strain generated by adduct formation. Intercalation is a natural DNA-binding mechanism, and a simple unwinding motion normally creates the pocket needed.[73] In contrast, creation of an *optimal* external binding site for a large, highly charged ligand such as H_2T4 would involve significant melting of the local DNA structure.[24] In the present context, the residual steric effect is the net repulsion energy that accrues in the final, fully reorganized adduct due to unfavorable interactions between host and guest atoms. The counterbalancing forces that drive adduct formation include Coulombic interactions between peripheral charges on the porphyrin and phosphate groups on the DNA backbone,[74] hydrophobic effects, van der Waals interactions,[75] and any charge-transfer stabilization associated with interactions between the π systems of the ligand and the host.[16]

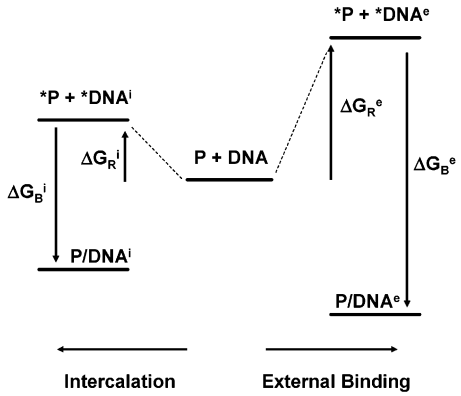

Figure 12. Qualitative energy diagram for competitive binding of H_2T4 to $[poly(dA-dT)]_2$. ΔG_R^e (ΔG_R^i) is the reorganization energy for external (intercalative) binding, and ΔG_B^e (ΔG_R^i) is the energy released upon external (intercalative) binding of preorganized species. The P + DNA state corresponds to the free components; an asterisk signifies reorganized for binding.

To summarize the arguments, it is convenient to use eq 3:

$$\Delta G = \Delta G_R + \Delta G_B \qquad (3)$$

where ΔG represents the interaction energy between the porphyrin and DNA, ΔG_R denotes the free energy needed to reorganize the DNA as well as the ligand, and ΔG_B is the free energy asssociated with the binding of the preorganized components.[16] Note that ΔG_B includes all terms that drive the binding as well as the steric strain. In Figure 12, the P + DNA state represents the unbound porphyrin and DNA. The ΔG_R^e term represents the free energy needed to prepare DNA and the porphyrin for external binding, and ΔG_B^e is the energy released upon formation of the externally bound adduct P/DNA^e. Likewise, the ΔG_R^i term represents the free energy needed to reorganize DNA and the porphyrin for intercalative binding, and ΔG_B^i is the energy released on formation of the intercalated adduct P/DNA^i. As drawn,

(69) Carvlin, M. J.; Mark, E.; Fiel, R.; Howard, J. C. *Nucleic Acids Res.* **1983**, *11*, 6141−6154.
(70) Sari, M. A.; Battioni, J. P.; Dupre, D.; Mansuy, D.; Lepecq, J. B. *Biochem. Pharmacol.* **1988**, *37*, 1861−1862.
(71) Tanious, F. A.; Yen, S. F.; Wilson, W. D. *Biochemistry* **1991**, *30*, 1813−1819.
(72) Bailly, C.; Graves, D. E.; Ridge, G.; Waring, M. J. *Biochemistry* **1994**, *33*, 8736−8745.
(73) Calladine, C. R.; Drew, H. R. *Understanding DNA*; Academic: New York, 1997.
(74) Sari, M. A.; Battioni, J. P.; Mansuy, D.; Lepecq, J. B. *Biochem. Biophys. Res. Commun.* **1986**, *141*, 643−649.
(75) Ren, J. S.; Jenkins, T. C.; Chaires, J. B. *Biochemistry* **2000**, *39*, 8439−8447.

Figure 12 provides a qualitative rationale for the fact that H_2T4 binds externally to $[poly(dA-dT)]_2$. Thus, the ease of melting $[poly(dA-dT)]_2$ permits formation of a very favorable external binding pocket that results in a highly exoergic ΔG_B^e. While the ΔG_R term is smaller for intercalation, strain reduces the free energy available for release during the ΔG_B^i step. The mix of factors therefore favors external binding. A discussion of a few other cases follows.

Case I. H_2T4 with $[Poly(dG-dC)]_2$: Robust hydrogen bonding in $[poly(dG-dC)]_2$ (or other DNA sequences rich in G≡C base pairs) disfavors effective external binding because the ΔG_R^e term is prohibitively endoergic.[25] As a consequence, the bulky H_2T4 ligand binds by intercalation despite steric strain in the minor groove that reduces the exoergonic character of the ΔG_B^i step.

Case II. H_2D4 with $[Poly(dA-dT)]_2$ or $[Poly(dG-dC)]_2$: The ΔG_B^i step is more negative for a dipyridylporphyrin because of the sharp reduction in steric strain in the minor groove of DNA. The charge of the cation may be another factor, but the bottom line is that intercalation is the preferred mode of binding regardless of the base composition of the DNA.

Case III. Zn(T4) with $[Poly(dG-dC)]_2$: Neither mode of binding is very favorable. As always with $[poly(dG-dC)]_2$, the ΔG_R^e term disfavors external binding because of the high reorganizational barrier. However, the ΔG_R^i is also less favorable because zinc must lose an axial ligand. The result is that both modes of uptake occur with intercalation being more competitive at low ionic strength,[64] but the binding constant is relatively small.[76]

Case IV. Zn(D4) with $[Poly(dA-dT)]_2$ or $[Poly(dG-dC)]_2$: Once again, the ΔG_B^i step becomes much more competitive relative to the ΔG_B^e step because of reduced strain in the intercalated form. As a result, intercalation becomes the preferred mode of binding, independent of the base composition of the DNA. However, the requirement for dissociation of an axial ligand from zinc enhances the ΔG_R^i term and decreases the binding affinity.

Conclusions

The dipyridylporphyrins H_2D3 and H_2D4 present no significant steric problems and freely intercalate into DNA sequences containing A=T *or* G≡C base pairs. By comparison with the quadruply charged H_2T4 system, the dipyridylporphyrins have less oxidizing excited states. For that reason, intercalation into $[poly(dG-dC)]_2$ does not quench the emission, but 5′-GpG-3′ steps appear to be weakly quenching.

The H_2D2 isomer also intercalates into $[poly(dG-dC)]_2$, but with a significantly lower binding constant. Frontal strain associated with the (*N*-methyl)pyridinium-2-yl groups destabilizes intercalated forms and may relegate H_2D2 to bind externally to $[poly(dA-dT)]_2$.

The zinc derivative Zn(D4) also acts as a universal intercalator and in the process suffers the loss of an axial ligand. This lowers the binding affinity and results in smaller spectral shifts for absorption and emission bands of the porphyrin. When Zn(D4) intercalates into $[poly(dA-dT)]_2$, the porphyrin emission actually shifts to higher energy.

Recognizing important structural considerations is key to a qualitative understanding of binding trends for cationic porphyrins. Steric clashes in the minor groove destabilize the intercalated form of tetrasubstituted porphyrins such as H_2T4.[18] On the other hand, the reorganizational energy suppresses external binding in DNA sequences that are rich in G≡C base pairs.

Acknowledgment. The National Science Foundation helped fund this research through Grant CHE 01-08902. The authors thank John Anderson, Christine A. Hyrcyna, Michael J. Scott, Arnold Stein, and Michael J. Therien for helpful suggestions as well as for access to equipment and materials. Michael A. Flory helped with attempts to synthesize dipyrromethane.

IC035092I

(76) Strickland, J. A.; Marzilli, L. G.; Gay, K. M.; Wilson, W. D. *Biochemistry* **1988**, *27*, 8870−8878.